Abstract

This study presents a comprehensive numerical investigation of lead-free Cs_2TiBr_6-based perovskite solar cells (PSCs) using SCAPS-1D simulation software. The research evaluates the effects of absorber thickness, interface defect densities, and the choice of electron and hole transport layers (ETLs and HTLs) on photovoltaic parameters. The optimal configuration, $Au/CuAlO_2/Cs_2TiBr_6/ZnO/FTO$, achieved a power conversion efficiency (PCE) of 19.53%, with a Voc of 1.123 V, Jsc of 23.54 mA/cm^2, and FF of 73.86%. These findings demonstrate the potential of Cs_2TiBr_6 as a sustainable and efficient alternative to lead-based perovskites, addressing critical environmental and health concerns while maintaining competitive performance.

1)Introduction

As the world's population grows, the demand for energy continues to rise, and our dependence on fossil fuels becomes increasingly unsustainable. The need for renewable energy solutions is more urgent than ever, with solar energy being one of the most promising alternatives due to its abundance and environmental benefits. Solar cells, or photovoltaics (PVs), convert sunlight into electricity, and over the years, they have become a key focus for addressing global energy demands.

Traditional silicon-based solar cells have been the dominant technology for decades. However, they come with some significant drawbacks, including high production costs, moderate efficiency, and complex manufacturing processes. These challenges have driven researchers to explore alternatives that could offer higher performance at a lower cost. One such alternative is perovskite solar cells (PSCs), which have gained significant attention in recent years due to their impressive efficiency and relatively low production costs.

Perovskite solar cells are based on materials that have a specific crystal structure known as ABX_3, where "A" is a cation, "B" is a metal cation, and "X" is a halide anion. These materials have several properties that make them excellent for solar energy conversion. They offer tunable bandgaps, which means they can be optimized for different types of sunlight. They also have low exciton binding energies (around 20 meV), long carrier diffusion lengths, and high light absorption coefficients, all of which contribute to their efficiency in capturing and converting light. These features make PSCs capable of harnessing a broad spectrum of sunlight.

Since their introduction, the efficiency of PSCs has improved dramatically, with the best devices now achieving efficiencies of over 22%. This rapid progress has been driven by advances in material engineering and new fabrication methods. However, despite their promise, lead-based PSCs face significant challenges, mainly due to the toxicity of lead. While lead is an excellent material for light absorption and charge transport, it poses serious environmental and health risks, making it unsuitable for widespread use.

To address these concerns, researchers have been exploring lead-free alternatives. Among these, titanium-based double perovskites, such as Cs_2TiBr_6, have shown great potential. These materials are non-toxic and offer many of the same advantageous properties as lead-based perovskites, such as high stability and good absorption of sunlight. By replacing lead with more environmentally friendly elements, like titanium, Cs_2TiBr_6 presents a promising solution to the toxicity issues of conventional PSCs while maintaining efficiency and stability.

This study focuses on Cs_2TiBr_6-based perovskite solar cells, using a numerical simulation approach to optimize key device parameters. The goal is to evaluate how the thickness of the absorber layer, the choice of electron and hole transport layers, and the density of defects at the interfaces affect the performance of the solar cells.

2)Theoretical Concept

To analyze and optimize the performance of Cs_2TiBr_6-based perovskite solar cells, we use **SCAPS-1D**, a simulation tool designed to model the behavior of photovoltaic devices. SCAPS-1D is a one-dimensional software that uses fundamental semiconductor physics to simulate the movement of charge carriers (electrons and holes) within the solar cell. The tool relies on core principles like **Poisson's equation**, **continuity equations**, and **drift-diffusion models** to predict device characteristics.

Poisson's Equation in Semiconductor Physics

Poisson's equation, which links the electrostatic potential within a material to the distribution of charge. This equation is fundamental in understanding how charge carriers behave within a semiconductor. In the context of a solar cell, Poisson's equation helps us determine the electric field and potential that drives the movement of charge carriers through the device:

$$\nabla^2\varphi(x) = -\frac{\rho(x)}{\varepsilon}$$

$\nabla^2\varphi(x)$: Laplacian of the electrostatic potential $\varphi(x)$
$\rho(x)$: Charge density at a point x
ε: Permittivity of the material

Charge Density in Semiconductors

The charge density is a critical parameter that determines the movement of charge carriers in a solar cell. In semiconductors, the charge density consists of the free electrons and holes, as well as the ionized donor and acceptor states. The charge density can be expressed as:

$$\rho(x) = q(p(x) - n(x) + (ND+) - (NA-)$$

Where:

- q is the elementary charge,
- p(x) and n(x) are the hole and electron concentrations, respectively,
- ND+ and NA− represent the ionized donor and acceptor concentrations.

Drift-Diffusion Model

The drift-diffusion model describes the transport of charge carriers under the influence of both electric fields and concentration gradients. This model helps to understand how the electrons and holes move through the semiconductor and contribute to the current. The current density for electrons (Jn) and holes (Jp) is described by both **drift** (movement due to the electric field) and **diffusion** (movement due to concentration gradients) components: It considers two primary mechanisms:

Drift: The motion of carriers under the influence of an electric field.
Diffusion: The movement of carriers from regions of high concentration to low concentration.

$$Jn(x) = q\,\mu n\, n(x)\varepsilon(x) + qDn\frac{\partial n(x)}{\partial x}$$

$$Jp(x) = q\mu p\, p(x)\varepsilon(x) - qDp\frac{\partial p(x)}{\partial x}$$

Where:

- q is the elementary charge,

- μn and μp are the electron and hole mobilities,
- n(x) and p(x)are the electron and hole concentrations,
- Dn and Dp are the electron and hole diffusion coefficients, and
- ε(x) is the electric field.

This model allows for the calculation of the current in the device and helps to understand how different material properties affect the overall device performance.

Performance Metrics

The performance of a solar cell is evaluated based on several key parameters:

- **Open-Circuit Voltage (Voc)**: The voltage across the device when no current is flowing.
- **Short-Circuit Current (Jsc)**: The current when the voltage is zero.
- **Fill Factor (FF)**: A measure of the quality of the solar cell's I-V curve. It represents the ratio of the actual maximum power to the theoretical maximum power.
- **Power Conversion Efficiency (PCE)**: The ratio of the output power to the input power. It is calculated using the formula:
- **Isc**: Short-circuit current (current when voltage is zero)

$$\eta = \frac{(Jsc * Voc * FF)}{Pin}$$

$$FF = \frac{(Pmax)}{(Voc * Isc)}$$

Where Pin is the input power (usually 1000 W/m² for AM1.5G light) and Pmax is the maximum output power.

Using SCAPS-1D, we simulate the effect of varying material properties such as bandgap, carrier mobility, and defect density, as well as structural factors like layer thickness, to optimize the performance of Cs_2TiBr_6-based solar cells. This approach allows for a detailed understanding of the factors that influence device efficiency and provides valuable insights into how to enhance performance for practical applications.

3. Materials and Methodology

This study focuses on the numerical design and optimization of high-performance Cs_2TiBr_6-based perovskite solar cells (PSCs) using SCAPS-1D simulation software. Cs_2TiBr_6, a lead-free titanium-based double perovskite, was chosen as the absorber material for its excellent optoelectronic properties, including a direct bandgap of 1.8 eV, high absorption coefficients, and superior environmental stability.

Device Structure

The simulated device configuration is a multilayer structure with the following composition:

- **Back Contact**: Gold (Au)
- **Hole Transport Layer (HTL)**: $CuAlO_2$
- **Absorber Layer**: Cs_2TiBr_6
- **Electron Transport Layer (ETL)**: ZnO
- **Transparent Conductive Oxide (TCO)**: Fluorine-doped Tin Oxide (FTO)

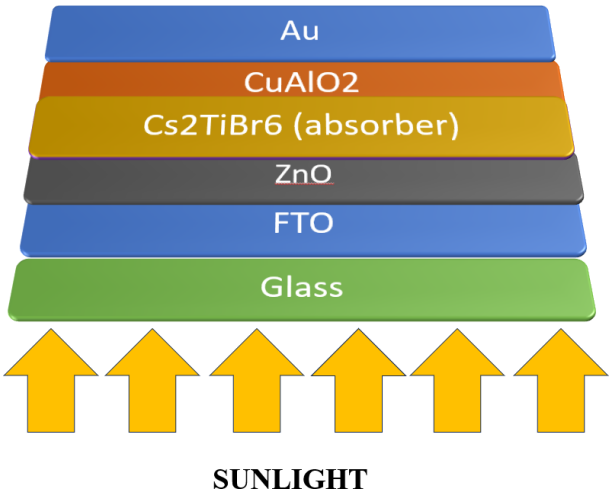

This structure is designed to maximize charge extraction while maintaining compatibility with the energy levels of the Cs_2TiBr_6 absorber.

Transport Layer Materials

The choice of HTL and ETL plays a crucial role in determining the efficiency and stability of the PSC. Various HTL and ETL materials were tested during the simulations to optimize the device performance. Based on the results:

- **HTL Candidates**: $CuAlO_2$ was selected for its excellent hole mobility, high thermal stability, and suitable energy alignment with the absorber layer.
- **ETL Candidates**: ZnO was identified as the optimal electron transport layer due to its high electron mobility, low recombination rate, and compatibility with Cs_2TiBr_6.

Simulation Parameters

The simulations were carried out under standard test conditions using the AM1.5G solar spectrum (1000 W/m^2) and a temperature of 300 K. SCAPS-1D was used to model the following parameters:

1. **Power Conversion Efficiency (PCE)**
2. **Open-Circuit Voltage (Voc)**
3. **Short-Circuit Current Density (Jsc)**
4. **Fill Factor (FF)**
5. **Quantum Efficiency (QE)**

TABLE 1 INPUT PARAMETERS OF ETLs

PARAMETERS	FTO	TiO2	Zno	STO	IGZO	PCBM	Znse	CdS	WO3
Thickness (nm)	500	30	30	30	30	30	30	30	30
BandGap , Eg(eV)	3.2	3.2	3.3	3.2	3.05	2	2.81	2.4	2.92
Electrno affinity X (eV)	4.4	3.9	4.1	4.0	4.16	3.9	4.09	4.18	4.590
Realtive Dielectric Permittivity	9	9	9	8.7	10	4	8.6	10	5.76
CB , Effective density of states Nc (cm-3)	$2.2X10^{18}$	$1X10^{21}$	$4X10^{18}$	$1.7X10^{19}$	$5X10^{18}$	$1X10^{21}$	$2.2X10^{18}$	$2.2X10^{18}$	$1.96X10^{19}$
VB , effective density of states Nv (cm-3)	$1.8X10^{19}$	$2X10^{20}$	$1X10^{19}$	$2X10^{20}$	$5X10^{18}$	$1.8X10^{19}$	$1.8X10^{18}$	$1.9X10^{19}$	$1.96E^{19}$
Electron mobility (cm2v-1s-1)	90	20	100	$5.3X10^{3}$	15	$1E^{-2}$	$4x10^{2}$	100	$1E^{+1}$
Hole mobility (cm2v-1s-1)	90	10	25	$6.6X10^{2}$	0.1	$1E^{-2}$	$1.1x10^{2}$	25	$1E^{+1}$
Shallow uniform donor density ND (cm-3)	$7X10^{2}$	$1X10^{19}$	$1X10^{18}$	$2X10^{16}$	$1X10^{18}$	$1E^{+20}$	$1x10^{18}$	$1X10^{18}$	$3.68E^{+19}$
Shallow acceptor density NA (cm-3)	0	0	0	0	0	0	0	0	0
Total defect density Nt (cm-3)	$1X10^{14}$	$1X10^{14}$	$1X10^{14}$	$1X10^{14}$	$1X10^{14}$	$1X10^{14}$	$1X10^{14}$	$1X10^{14}$	$1X10^{14}$

TABLE 2 INPUT PARAMETERS OF HTLs.

PARAMETERS	Cu20	CuAlO2	CuSbS2	CuSCN	MoO3	Spiro-OMeTAD	P3HT	PEDOT:PSS	Cs2TiBr6
Thickness (nm)	30	30	30	30	30	30	30	30	900
BandGap , Eg(eV)	2.17	3.46	1.58	3.2	3	3	1.85	2.2	1.6
Electrno affinity X (eV)	3.2	2.5	4.2	1.9	2.5	2.45	3.1	2.9	4.47
Realtive Dielectric Permittivity	7.1	60	14.6	10	12.5	3	3.4	3	10
CB , Effective density of states Nc (cm-3)	$2.02x10^{17}$	$2.2X10^{18}$	$2X10^{18}$	$2.2X10^{19}$	$2.2X10^{18}$	$1X10^{19}$	$1E^{+22}$	$2.2E^{+15}$	$1E^{19}$

VB , effective density of states Nv (cm-3)	$1.1x10^{19}$	$1.8X10^{19}$	$1X10^{-4}$	$1.8X10^{19}$	$1.8X10^{19}$	$1X10^{19}$	$1E^{+22}$	$2.2E^{+17}$	$1E^{19}$
Electron mobility (cm2v-1s-1)	200	2	49	$1X10^{-4}$	100	$2X10^{-4}$	$1E^{-4}$	$2X10^{-3}$	4.4
Hole mobility (cm2v-1s-1)	80	8.6	49	$1X10^{-1}$	25	$2X10^{-4}$	$1E^{-4}$	$2X10^{-3}$	2.5
Shallow uniform donor density ND (cm-3)	0	0	0	0	0	0	0	0	$1E^{+19}$
Shallow acceptor density NA (cm-3)	$9 X 10^{21}$	$3 X 10^{18}$	$1.38X^{18}$	$1X10^{15}$	$1X10^{18}$	$2X10^{18}$	$3.17E^{13}$	$1E^{+17}$	$1E^{+19}$
Total defect density Nt (cm-3)	$1 X 10^{14}$	$1X 10^{14}$	$1 X 10^{14}$	$1 X 10^{14}$	$1 X 10^{14}$	$1 X 10^{14}$	$1 X 10^{14}$	$1 X 10^{14}$	$1 X 10^{14}$

Table 3 . Input Parameters of Interface Defect and Absorber Defect.

Parameters and units	Cs2TiBr6	ETL/Cs2TiBr6 interface	Cs2TiBr6 / HTL interface
DEFECT TYPE	NEUTRAL	Acceptor	Acceptor
Capture cross section for electron and holes (cm2)	$2.0X10^{-14}$, $2X10^{-14}$	$1.0X10^{-17}$, $1X10^{-18}$	$1.0X10^{-18}$, $1X10^{-19}$
Energetic distribution	GAUSSIAN	SINGLE	SINGLE
Energy level with respect to EV (above EV , eV)	0.6	0.6	0.6
Characteristics energy (eV)	0.1	-	-
Total Density (cm-3)	$1.0 X 10^{13}$	$1.0 X 10^{10}$ - $1.0 X 10^{12}$	$1.0 X 10^{10}$ - $1.0 X 10^{12}$

OPTIMIZATION PARAMETERS

Several parameters were varied during the simulations to identify the optimal device configuration:

1. **Absorber Thickness**: The thickness of the Cs_2TiBr_6 layer was varied from 100 nm to 1300 nm to determine its impact on light absorption, carrier transport, and overall efficiency.
2. **Interface Defect Density**: The defect densities at the Cs_2TiBr_6/HTL and Cs_2TiBr_6/ETL interfaces were varied to analyze their effect on charge recombination and device performance.
3. **Transport Layer Thickness**: The thickness of the HTL and ETL layers was adjusted to optimize charge extraction and minimize series resistance.

MATERIAL PARAMETERS

The physical and electronic properties of the materials used in the simulations are summarized below:

Parameter	FTO	ZnO	$CuAlO_2$	Cs_2TiBr_6
Thickness (nm)	500	30	30	900
Bandgap, Eg (eV)	3.5	3.3	3.1	1.8
Electron Affinity, χ (eV)	4.4	4.1	4.07	4.47
Dielectric Permittivity, εr	9	9	7.11	10
Electron Mobility, μ_n ($cm^2 \cdot V^{-1} \cdot s^{-1}$)	20	100	200	1.6
Hole Mobility, μ_h ($cm^2 \cdot V^{-1} \cdot s^{-1}$)	10	25	8600	1.6
Defect Density, Nt (cm^{-3})	--	10^{14}	10^{14}	10^{13}

SIMULATION WORKFLOW

1. **Initial Configuration**: The baseline device structure was configured with standard values for absorber thickness (900 nm), transport layer thickness (30–100 nm), and interface defect density (10^{13}–10^{14} cm^{-3}).
2. **Parameter Variation**: Key parameters, including absorber thickness, defect densities, and transport layer combinations, were systematically varied to evaluate their impact on performance metrics.
3. **Performance Evaluation**: The resulting devices were evaluated based on PCE, Voc, Jsc, FF, and QE, with the best-performing configuration identified as $Au/CuAlO_2/Cs_2TiBr_6/ZnO/FTO$.

4) RESULTS AND DISCUSSION

The performance of Cs_2TiBr_6-based perovskite solar cells (PSCs) was analyzed by systematically varying critical parameters such as absorber thickness and operating temperature. These variations provided insights into the behavior of key photovoltaic metrics, including short-circuit current density (Jsc), open-circuit voltage (Voc), power conversion efficiency (PCE), and fill factor (FF). The results are discussed in detail below.

4.1. Effect of Absorber Thickness

The thickness of the Cs_2TiBr_6 absorber layer is a crucial factor in determining the overall efficiency of the solar cell. A thicker absorber layer enhances light absorption, resulting in higher Jsc. However, beyond an optimal thickness, excessive material can increase recombination losses and reduce carrier mobility, which negatively impacts Voc, FF, and ultimately PCE.

- **Jsc (Short-Circuit Current Density)**:
  As the thickness of the Cs_2TiBr_6 absorber increased, Jsc initially rose due to improved photon absorption and enhanced carrier generation. The graph showed a steep increase in Jsc at lower thickness values, reaching a saturation point at around 900 nm. Beyond this thickness, additional material did not significantly enhance light capture, as most incident photons had already been absorbed.

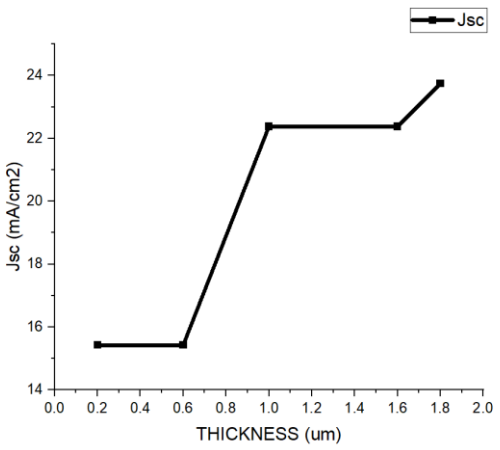

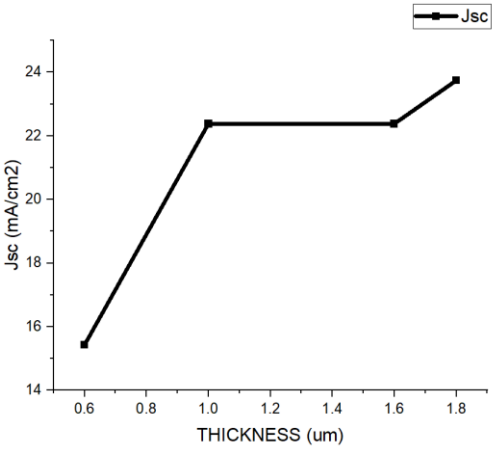

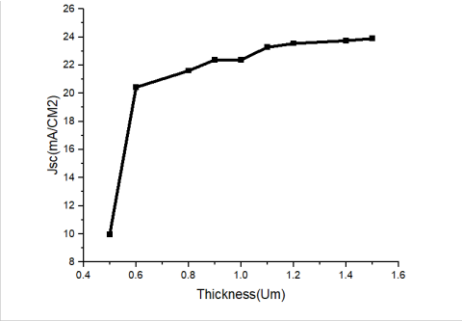

- **PCE (Power Conversion Efficiency)**:
  PCE followed a similar trend to Jsc, increasing rapidly with thickness initially and then leveling off. The maximum PCE of 19.53% was achieved at an absorber thickness of 900 nm. Further increases in thickness led to recombination losses and resistive effects, resulting in a gradual decline in efficiency.

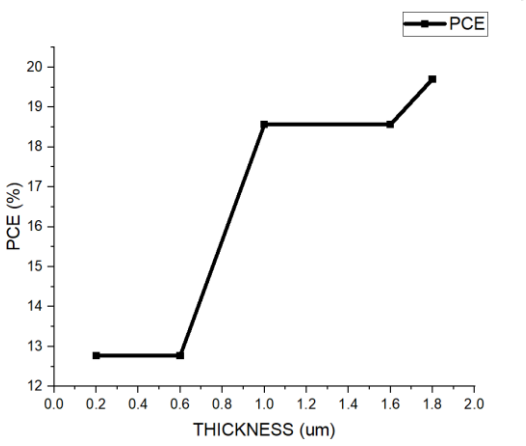

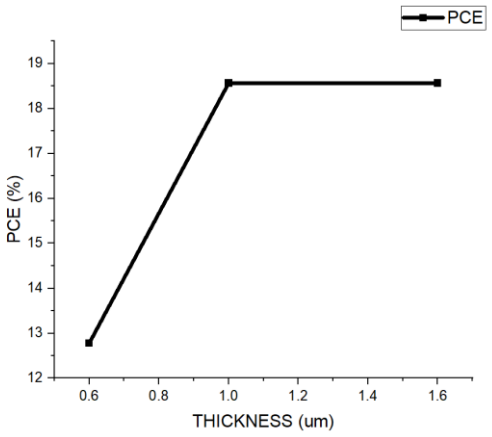

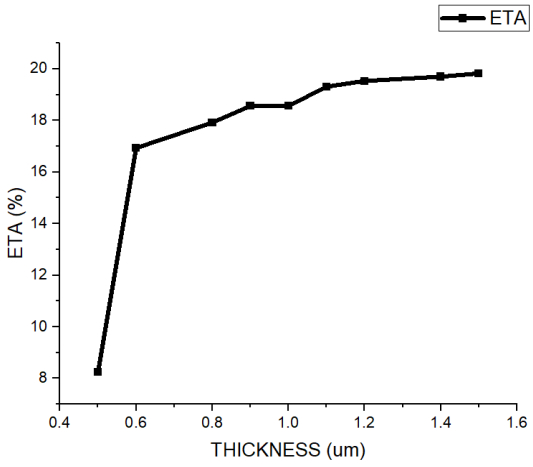

- **Voc (Open-Circuit Voltage)**:
  Voc was inversely affected by absorber thickness. As the thickness grew, the increased recombination rate at the bulk and interfaces caused a reduction in the effective voltage sustained across the cell. This behavior highlights the trade-off between Jsc and Voc with varying thickness.

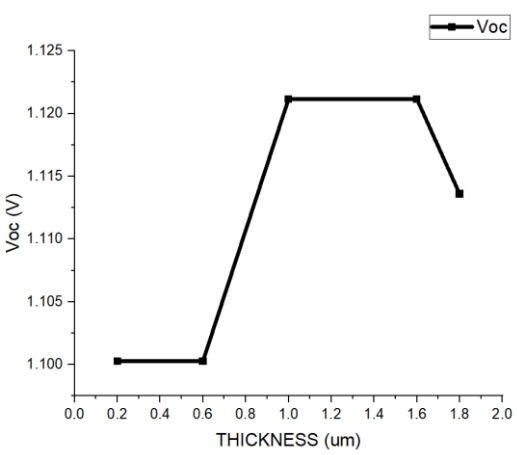

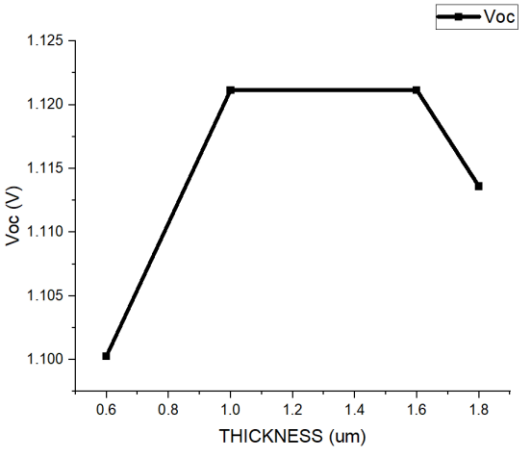

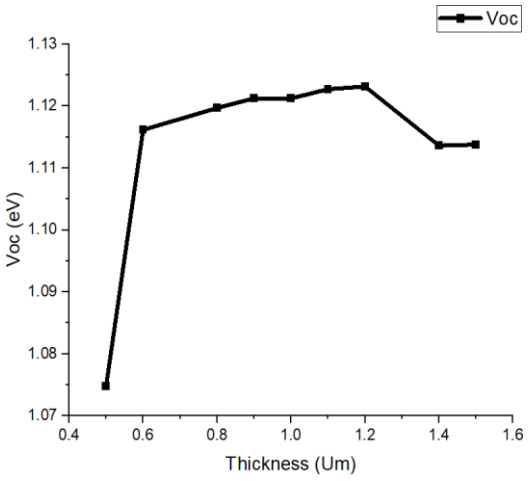

- **FF (Fill Factor)**:
  FF exhibited a declining trend with increasing thickness due to higher resistive losses and reduced carrier extraction efficiency. Thicker layers also increased the likelihood of charge trapping and recombination, further reducing FF.

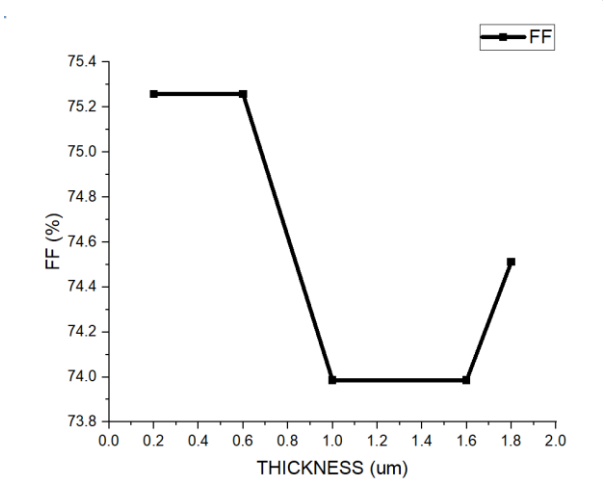

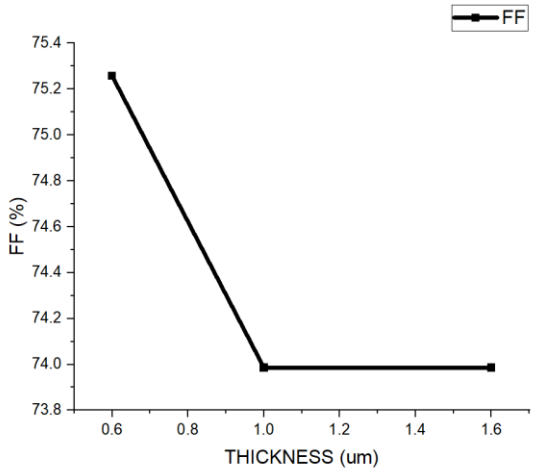

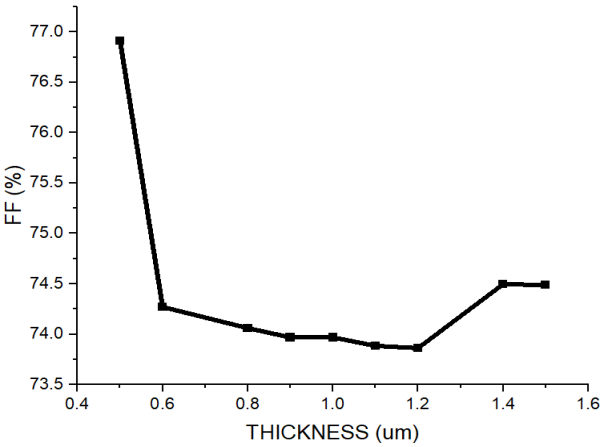

Optimal Thickness:
The simulations identified an absorber thickness of 900 nm as optimal for the Cs_2TiBr_6 PSC, balancing light absorption with charge transport and recombination dynamics.

4.2. Effect of Temperature

The temperature sensitivity of Cs_2TiBr_6-based PSCs was evaluated over a range of 300 K to 450 K. Temperature significantly influenced the key photovoltaic parameters, as outlined below:

- **Jsc (Short-Circuit Current Density)**:
  Jsc showed a slight increase with rising temperature due to enhanced thermal energy, which generated additional charge carriers. However, the impact on overall performance was minimal, as recombination losses at higher temperatures offset these gains.

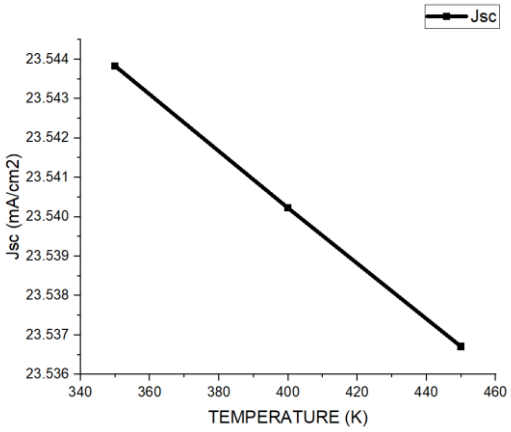

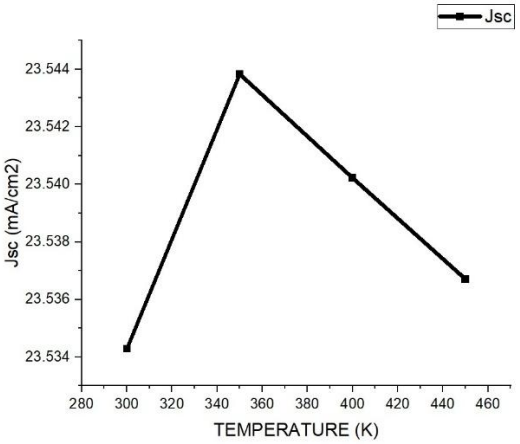

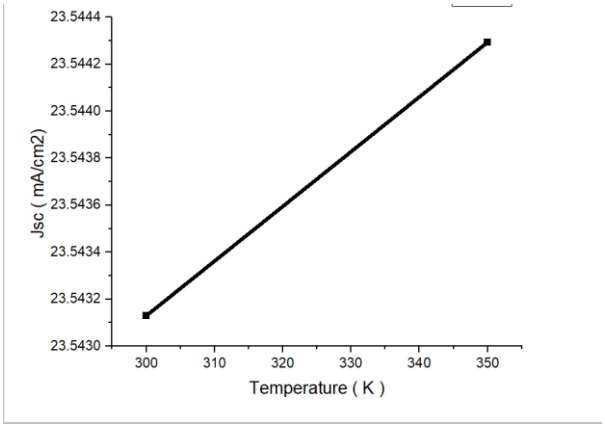

- **Voc (Open-Circuit Voltage)**:
  Voc decreased significantly with temperature due to the narrowing of the semiconductor bandgap. This reduction in bandgap lowered the maximum achievable voltage, which is a critical factor in determining overall efficiency.

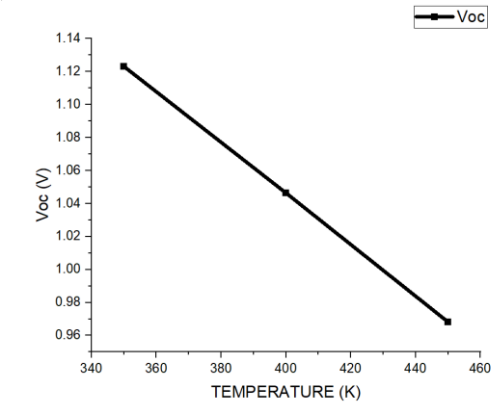

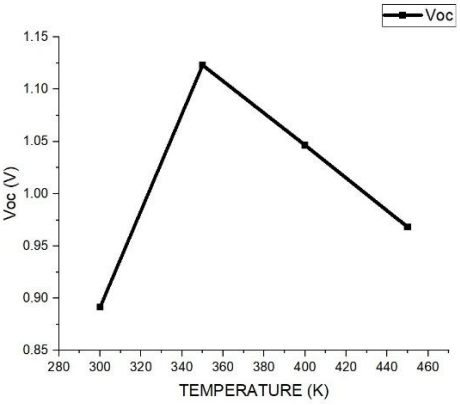

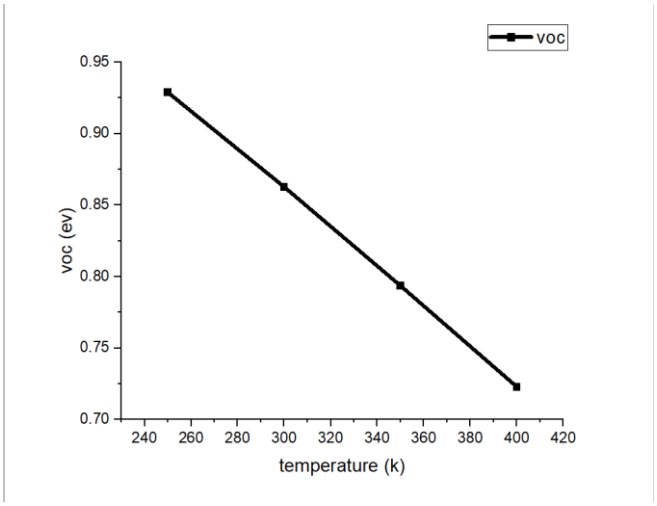

- **PCE (Power Conversion Efficiency)**:
  PCE declined with increasing temperature as the loss in Voc outweighed the minor gains in Jsc. At elevated temperatures, the combined effects of reduced voltage, increased recombination rates, and resistive losses resulted in a noticeable drop in efficiency.

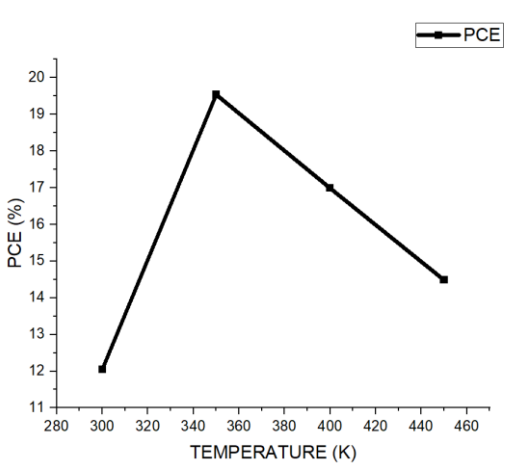

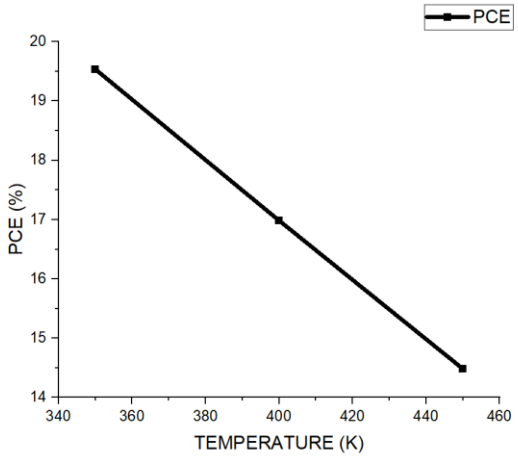

- **FF (Fill Factor)**:
  FF also decreased with temperature, driven by higher recombination rates and resistive effects. The deterioration in FF reflects the reduced ability of the cell to efficiently extract and transport charge carriers at higher temperatures.

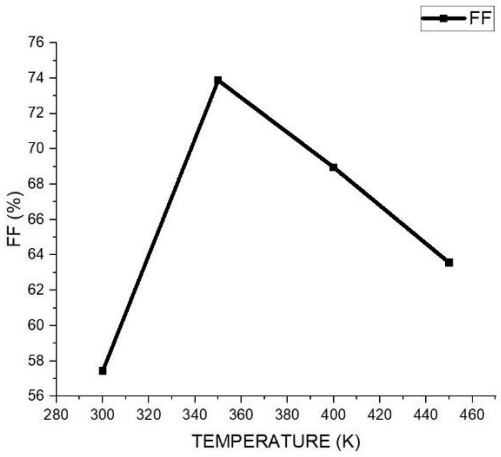

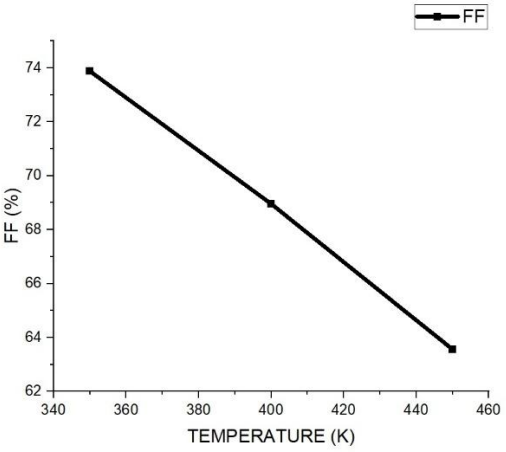

Thermal Performance:
The simulations highlighted the importance of effective thermal management strategies, such as the incorporation of cooling systems or heat sinks, to maintain device stability and efficiency under varying operating conditions.

4.3. KEY OBSERVATIONS

1. **Absorber Thickness Optimization**:
   - Optimal thickness: 900 nm
   - PCE: 19.53%
   - Voc: 1.123 V
   - Jsc: 23.54 mA/cm²
   - FF: 73.86%
2. **Temperature Sensitivity**:
   - Operating temperature range: 300–450 K
   - Significant decline in Voc and FF at higher temperatures highlights the need for thermal stability improvements.
3. **Impact of Interface Defects**:
   The role of interface defect density was also evaluated, with lower defect densities (<10^13 cm−3) resulting in significantly improved performance. This underscores the importance of high-quality fabrication techniques to minimize defects and enhance overall efficiency.

This analysis confirms the potential of Cs_2TiBr_6 as a high-performance, lead-free absorber material for PSCs. While achieving a competitive efficiency of 19.53%, further improvements in thermal stability and defect management could push the performance of these cells even higher.

iv) Energy Level vs Thickness

The energy levels of the materials, particularly the conduction band and valence band positions, are critical for efficient charge separation and transport. For Cs_2TiBr_6-based perovskite solar cells, the alignment of these energy levels with the transport layers (ZnO as ETL and $CuAlO_2$ as HTL) ensures minimal energy barriers and effective charge extraction.

As the thickness of the Cs_2TiBr_6 absorber layer changes, it influences the potential barriers at the interfaces, affecting carrier transport. Thinner layers reduce the distance carriers must travel, improving charge collection efficiency. However, excessively thin layers can increase recombination losses due to incomplete photon absorption. Conversely, thicker layers improve light absorption but may result in higher resistive losses and reduced carrier mobility if the energy level alignment and transport properties are not optimized.

The simulation results indicated that an optimal thickness of 900 nm for Cs_2TiBr_6 achieves the best balance between light absorption and charge transport. At this thickness, the energy levels of Cs_2TiBr_6 align well with ZnO and $CuAlO_2$, facilitating efficient carrier extraction and reducing recombination losses.

v) Quantum Efficiency vs wavelength

The quantum efficiency (QE) of Cs_2TiBr_6-based PSCs was analyzed across the UV, visible, and near-infrared (NIR) regions of the solar spectrum. The findings highlight the wavelength-dependent absorption capabilities of Cs_2TiBr_6:

1. **UV Range (100–400 nm)**:
   The QE in the UV region was relatively low, reflecting Cs_2TiBr_6's limited ability to absorb high-energy photons. This behavior is typical of most perovskites, as the material's bandgap does not favor efficient photon conversion in this range.
2. **Visible Range (400–700 nm)**:
   The QE peaked in the visible region, demonstrating Cs_2TiBr_6's high efficiency in absorbing and converting photons into charge carriers. This range aligns with the material's direct bandgap of ~1.8 eV, making it well-suited for visible light absorption.
3. **Near-Infrared Range (700–1100 nm)**:
   The QE declined gradually in the NIR region as the photon energy dropped below the material's bandgap. However, Cs_2TiBr_6 maintained moderate absorption in this range, indicating its potential for tandem applications when paired with lower bandgap materials.

vi) Optimization of PCE from Layer-Wise (Perovskite, Hole Transport Layer, Electron Transport Layer)

Achieving high power conversion efficiency (PCE) in Cs_2TiBr_6-based PSCs requires optimizing the absorber layer, electron transport layer (ETL), and hole transport layer (HTL). Each layer plays a vital role in charge generation, transport, and extraction:

1. **Perovskite Layer (Cs_2TiBr_6)**:
   The absorber thickness was optimized at 900 nm, which balanced high photon absorption with efficient charge transport. This configuration maximized light absorption while minimizing recombination losses, leading to the highest observed PCE of 19.53%.

2. **Electron Transport Layer (ZnO)**:
   ZnO was selected as the ETL due to its high electron mobility and excellent energy alignment with Cs_2TiBr_6. This combination minimized resistive losses and enhanced electron extraction efficiency.
3. **Hole Transport Layer ($CuAlO_2$)**:
   $CuAlO_2$ provided high hole mobility and stable energy alignment with Cs_2TiBr_6. Its thermal and chemical stability also improved the overall stability of the device, making it a reliable choice for long-term operation.

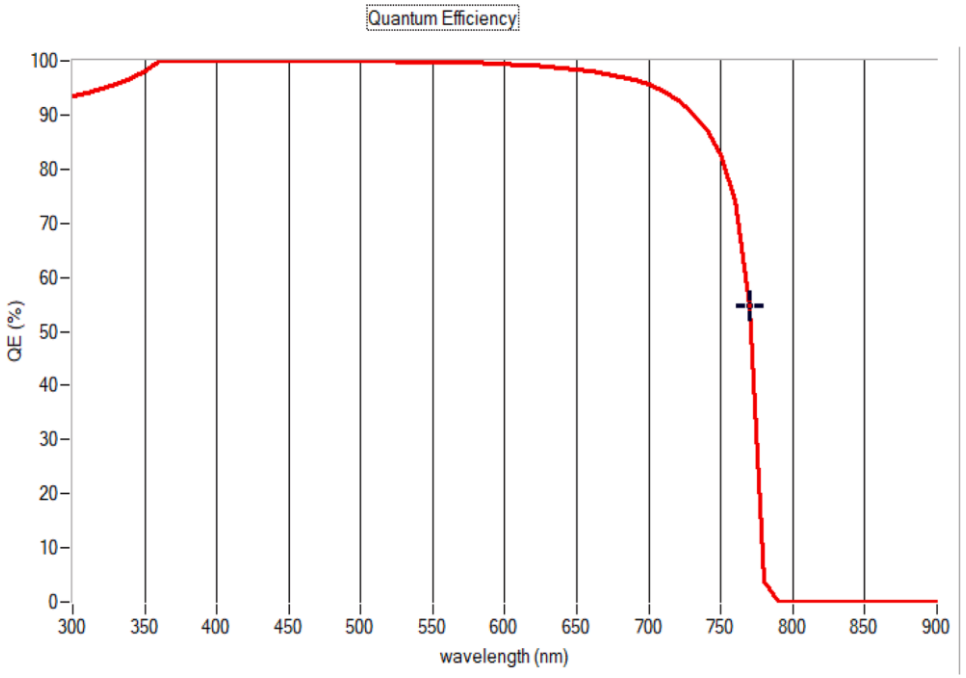

4.4. Device Structure Optimization

Simulations of various combinations of ETLs and HTLs were performed to identify the optimal configuration for Cs_2TiBr_6-based PSCs. The structure $Au/CuAlO_2/Cs_2TiBr_6/ZnO/FTO$ achieved the best performance metrics, as summarized below:

Structure of PSCs	Voc (V)	Jsc (mA/cm2)	FF (%)	PCE(%)
Au/ CUALO2 / Cs2TiBr6 / IGZO/FTO	1.1231	23.543828	73.88	19.53
Au/ CUALO2 / Cs2TiBr6 / ZNO/FTO	1.1231	23.543129	73.86	19.53
Au/ CUALO2 / Cs2TiBr6 / TIO2/FTO	1.1267	23.546622	72.46	19.22
Au/ CU2O / Cs2TiBr6 / ZNSE/FTO	0.6726	23.54986	69.26	10.97
Au/CU2O/ Cs2TiBr6 / PCBM/FTO	0.6732	23.551993	68.38	10.84
Au/ CU2O / Cs2TiBr6 / TIO2/FTO	0.6727	23.549836	67.41	10.68
Au/ CU2O / Cs2TiBr6 / ZNO/FTO	0.6614	24.16615	64.38	10.29
Au/ MOO3 / Cs2TiBr6 / CDS/FTO	0.6582	23.551529	60.16	9.33
Au/ MOO3 / Cs2TiBr6 / ZNO/FTO	0.6579	23.546039	60.16	9.32
Au/ MOO3 / Cs2TiBr6 / TIO2/FTO	0.6582	23.549529	58.43	9.06
Au/ SPIRO -OMeTAD / Cs2TiBr6 / ZNSE/FTO	0.634	23.549901	59.81	8.93

Au/ SPIRO -OMeTAD / Cs2TiBr6 / PCBM/FTO	0.6347	23.551731	58.95	8.81
Au/ CUALO2 / Cs2TiBr6 / STO/FTO	1.1205	15.904997	41.44	7.39
Au/ PEDOT:PSS / Cs2TiBr6 / CDS/FTO	0.383	23.546106	43.23	3.9
Au/ PEDOT:PSS / Cs2TiBr6 / IGZO/FTO	0.3828	23.541682	43.24	3.9
Au/ PEDOT:PSS / Cs2TiBr6 / TIO2/FTO	0.383	23.535408	40.99	3.69
Au/ CUSCN / Cs2TiBr6 / CDS/FTO	0.2609	22.975117	30.1	1.8
Au/ CUSCN / Cs2TiBr6 / ZNO/FTO	0.2607	22.96727	30.09	1.8
Au/ CUSCN / Cs2TiBr6 / ZNSE/FTO	0.2609	22.966359	30.04	1.8
Au/ CUSCN / Cs2TiBr6 / TIO2/FTO	0.261	22.692913	28.3	1.68
Au/CU2O/ Cs2TiBr6 / STO/FTO	0.6879	1.058673	30.1	0.22
Au/ MOO3 / Cs2TiBr6 / STO/FTO	0.6719	1.050232	29.72	0.21
Au/ SPIRO -OMeTAD / Cs2TiBr6 / STO/FTO	0.649	1.019989	29.12	0.19
Au/ PEDOT:PSS / Cs2TiBr6 / STO/FTO	0.3936	7.62E-01	16.52	0.05
Au/ CUSCN / Cs2TiBr6 / STO/FTO	0.2745	4.03E-01	16.62	0.02
Au/ P3HT / Cs2TiBr6 / STO/FTO	0.0362	5.55E-02	28.86	0
Au/ P3HT / Cs2TiBr6 / TIO2/FTO	0.0244	2.97E-01	22.75	0
Au/ P3HT / Cs2TiBr6 / ZNO/FTO	0.0241	2.97E-01	22.74	0

SS**Key Observations:**

- The structure with **$CuAlO_2$ as HTL** and **ZnO as ETL** delivered the highest PCE of 19.53%, due to its superior charge transport and reduced recombination losses.
- Replacing $CuAlO_2$ with alternative HTLs (e.g., CuO, PEDOT:PSS) resulted in lower PCE due to poorer hole mobility and less favorable energy alignment.
- The combination of ZnO as ETL with Cs_2TiBr_6 as the absorber consistently demonstrated high Jsc values, confirming its suitability for efficient electron transport.

5 CONCLUSION

5.1. Summary of Findings

This study focused on the design and optimization of cesium titanium bromide (Cs_2TiBr_6)-based perovskite solar cells (PSCs) as a sustainable and efficient lead-free alternative. The findings highlight the potential of Cs_2TiBr_6 for photovoltaic applications:

- **Cs_2TiBr_6 PSCs** achieved a power conversion efficiency (PCE) of 19.53%, balancing high efficiency with excellent thermal and chemical stability.
- The optimal device configuration, Au/$CuAlO_2$/Cs_2TiBr_6/ZnO/FTO, demonstrated superior performance due to effective energy alignment and reduced recombination losses.
- Thickness optimization revealed that a Cs_2TiBr_6 absorber thickness of 900 nm maximized light absorption and charge transport, ensuring peak device efficiency.
- Temperature analysis emphasized the need for thermal management to maintain stable operation under real-world conditions.

These results position Cs_2TiBr_6 as a viable lead-free material, offering a promising pathway toward environmentally friendly PSCs

5.2. Contributions of the Project

This research made significant contributions to the field of perovskite solar cells by:

1. Demonstrating the potential of Cs_2TiBr_6 as an efficient and stable lead-free absorber material for PSCs.
2. Providing a detailed optimization framework for absorber thickness, transport layers, and interface properties to enhance device performance.
3. Supporting the shift toward environmentally sustainable photovoltaic technologies by reducing reliance on toxic lead-based materials.
4. Highlighting the critical role of material properties, such as defect density and energy level alignment, in achieving high efficiency.

5.3. Future Work and Recommendations

While this study establishes Cs_2TiBr_6 as a promising material, further work is needed to address challenges and improve its competitiveness in the photovoltaic market. Future research should focus on:

1. **Improving Stability**: Develop strategies to enhance the long-term thermal and environmental stability of Cs_2TiBr_6 under outdoor operating conditions.

2. **Transport Layer Advancements**: Optimize electron and hole transport layers to improve charge mobility and reduce recombination losses.
3. **Scaling Fabrication**: Explore cost-effective and scalable manufacturing techniques to support the commercial adoption of Cs_2TiBr_6-based PSCs.
4. **Tandem Solar Cells**: Investigate the integration of Cs_2TiBr_6 into tandem cell architectures to achieve higher efficiencies by leveraging complementary bandgaps.
5. **Efficiency Improvements**: Bridge the efficiency gap between Cs_2TiBr_6 and conventional lead-based PSCs through innovative material engineering and doping techniques.
6. **Durability Testing**: Conduct extended durability and stability tests to validate the real-world performance of Cs_2TiBr_6-based devices.
7. **Economic Analysis**: Perform detailed cost-benefit analyses to evaluate the commercial viability of lead-free PSCs in large-scale deployments.

VI REFERENCES

1. **P. Arockia Michael Mercy** [*], **K.S. Joseph Wilson ,** *PG & Research Department of Physics, Arul Anandar College, Madurai Kamaraj University, Madurai, 625514, Tamilnadu, India*
2. • **Liu, F., & Chen, Y. (2023).** An optimization of Cs_2TiBr_6 perovskite solar cell using SCAPS-1D and genetic algorithm. *Canadian Journal of Chemical Engineering*, 101(4), 25315.
3. • **Kumar, S., Alam, I., Kushwaha, A. K., & Singh, S. V. (2021).** Investigating the theoretical performance of Cs_2TiBr_6-based perovskite solar cell with La-doped $BaSnO_3$ and $CuSbS_2$ as the charge transport layers. *arXiv preprint arXiv:2111.14381*.
4. • **Hosen, R., Sikder, S., Uddin, M. S., Haque, M. M., Mamur, H., & Bhuiyan, M. R. A. (2023).** Effect of various layers on improving the photovoltaic efficiency of Al/ZnO/CdS/CdTe/Cu_2O/Ni solar cells. *Journal of Alloys and Metallurgical Systems*, 4, 100041.
5. • **Rahman, M. Y., & Mominuzzaman, S. M. (2024).** Exploring Lead Free Mixed Halide Double Perovskites Solar Cell. *arXiv preprint arXiv:2401.09584*.
6. • **Brabec, C. J. (2023).** World record in solar energy. *Friedrich-Alexander-Universität Erlangen-Nürnberg (FAU)*.
7. • **Wang, Y., Mahmoudi, T., Rho, W.-Y., Yang, H.-Y., & Seo, S. (2017).** Ambient-air-solution-processed efficient and highly stable perovskite solar cells based on $CH_3NH_3PbI_3{-}xCl_x$-NiO composite with Al_2O_3/NiO interfacial engineering. *Nano Energy*, 40, 408-417.
8. • **Ahmad, K., & Kim, H. (2023).** Improved photovoltaic performance and stability of perovskite solar cells with device structure of (ITO/SnO_2/$CH_3NH_3PbI_3$/rGO+spiro-MeOTAD/Au). *Materials Science and Engineering: B*, 286, 116227.
9. • **Bi, E., Chen, H., Xie, F., Wu, Y., Chen, W., Su, Y., Islam, A., Grätzel, M., & Han, L. (2017).** Diffusion engineering of ions and charge carriers for stable efficient perovskite solar cells. *Nature Communications*, 8, 15330.
10. • **Tang, X., van den Berg, M., Gu, E., Horneber, A., Matt, G. J., Osvet, A., Bein, T., Docampo, P., Brabec, C. J., & Spiecker, E. (2018).** Local Observation of Phase Segregation in Mixed-Halide Perovskite. *Nano Letters*, 18(3), 2172-2178.
11. • **Shrestha, S., Fischer, R., Matt, G. J., Feldner, P., Michel, T., Osvet, A., Levchuk, I., Merle, B., Golkar, S., Chen, H., Tedde, S. F., Hofer, F., Hock, R., & Brabec, C. J. (2017).** High-performance direct conversion X-ray detectors based on sintered hybrid lead triiodide perovskite wafers. *Nature Photonics*, 11, 436-440.